Influence of yttrium substitution on the magnetic and transport properties of UCu_5

2001 J. Phys.: Condens. Matter 13 4221

(http://iopscience.iop.org/0953-8984/13/19/304)

INSTITUTE OF PHYSICS PUBLISHING JOURNAL OF PHYSICS: CONDENSED MATTER

J. Phys.: Condens. Matter **13** (2001) 4221–4238 www.iop.org/Journals/cm PII: S0953-8984(01)19231-3

Influence of yttrium substitution on the magnetic and transport properties of UCu_5

M Ellerby[1,4], K A McEwen[1], M Watmough[1], M A López de la Torre[2], L Naber[3] and E Bauer[3]

[1] Department of Physics and Astronomy, University College London, Gower Street, London WC1E 6BT, UK
[2] Departamento de Fisica Aplicada, Facultad de Quimicas, Universidad de Castilla–La Mancha, 13071 Ciudad Real, Spain
[3] Institüt für Experimentalphysik, Technishe Universität Wien, Wiedner Hauptstasse, A-1040 Wien, Austria

E-mail: mark.ellerby@ucl.ac.uk

Received 21 November 2000, in final form 23 February 2001

Abstract

We have measured the resistivity, magnetoresistance, resistivity under hydrostatic pressure and the magnetization of the compound $(U_{1-x}Y_x)Cu_5$ for temperatures between 0.4 and 300 K, fields of up to 12 T and at pressures between 1 bar and 14 kbar. From this series of measurements we have derived compositional, H–T and p–T phase diagrams. Using thermodynamic arguments and a comparison of these phase diagrams we arrive at a nomenclature for the various phases which is consistent with that used for the parent compound UCu_5. We observe that the $1-q$ structure observed below $T_2 = 1.16$ K in UCu_5 is stabilized with increasing yttrium. In addition the introduction of yttrium results in a rapid reduction of T_N. The effects of 'chemical' pressure are found to be opposite to those observed for hydrostatic pressure, which enhances T_N and reduces T_2. From an analysis of the dc susceptibility we derive values for χ_0 (Pauli susceptibility) which indicate a large reduction of the density of states for $x > 0.1$ and this is consistent with the reduction of the resistivity observed at room temperature. However, this analysis could not rule out the possibility of a change in the source of the Kondo contribution. An analysis of the resistivity and Θ_P (paramagnetic Curie–Weiss temperature) for $(U_{0.7}Y_{0.3})Cu_5$ is consistent with the onset of a Kondo process with increasing yttrium doping.

[4] Author to whom correspondence should be addressed: Dr Mark Ellerby, Department of Physics and Astronomy, University College London, Gower Street, London WC1E 6BT, UK.

1. Introduction

UCu_5 is a particularly interesting intermetallic compound since it exhibits heavy fermion properties within a high moment ordered phase [1]. At $T_N = 16$ K, UCu_5 undergoes a second-order antiferromagnetic transition: Murasik *et al* [2] and Schenck *et al* [3] identified this structure as being a type-II antiferromagnet with a modulation wavevector $\boldsymbol{q} = (1/2, 1/2, 1/2)$. The moments within the (111) planes of the cubic $AuBe_5$ crystallographic structure are ferromagnetically aligned. The ordered moment in this phase has been reported as 0.9 [2] and 1.55 [3] μ_B/U atom. At a lower temperature, here denoted by $T_2 = 1.16$ K, a first order transition is observed [1], but Schenck *et al* [3] were unable to observe any evidence for a change in magnetic structure at T_2.

Nakamura *et al* [4] interpreted their nuclear magnetic resonance measurements in terms of a $4 - \boldsymbol{q}$ magnetic structure below T_N. They proposed that below T_2 the structure rearranges to form a multidomain $1 - \boldsymbol{q}$ structure. Subsequently Lopez de la Torre *et al* [5] made a detailed study of the magnetization of UCu_5, and presented thermodynamic arguments in support of the $4 - \boldsymbol{q}$ to $1 - \boldsymbol{q}$ model.

Metallurgical problems exist in making a single crystal of UCu_5 and all the studies reported have employed polycrystalline samples. In recent years attention has focused on the influence of doping on the two crystallographically distinct copper sites: the 4c sites have cubic symmetry ($\bar{4}3m$) whilst the 16e sites have trigonal symmetry ($3m$). For example, the substitution of Ag [6] on the 4c sites enhances the magnetic exchange, whilst doping with Pd [7] or Ni [8] suppresses the magnetic order. In the latter examples the magnetic, transport and thermal properties are inconsistent with Fermi-liquid behaviour at low temperatures [9, 10].

One of the most remarkable properties of UCu_5 is the huge increase (typically by a factor of five [5]) in its electrical resistivity that occurs as the sample temperature is reduced below T_2. Changes in resistivity at antiferromagnetic phase transitions are normally attributed to the changes in the Fermi surface which arise from the additional magnetic superzone boundaries that appear below the phase transition. However, it is rather surprising that the change from $4 - \boldsymbol{q}$ to $1 - \boldsymbol{q}$ structures should produce such a dramatic reduction in the Fermi surface. An alternative possible explanation for the resistivity increase could be that the electronic density of states varies unusually rapidly with energy in the region of the Fermi level. The present study of the effects of partial substitution on the U sites in UCu_5 was initially motivated by the desire to investigate the robustness of the resistivity increase at T_2 when the system was perturbed in this way.

We chose to substitute Y for U because of the chemical similarity of the elements. Since Y is nonmagnetic, we anticipate that the delicate balance between the free energies of the $4 - \boldsymbol{q}$ and $1 - \boldsymbol{q}$ structures is likely to be perturbed. Moreover, although U in UCu_5 has a mixed U^{3+}–U^{4+} valence character, its replacement by Y^{3+} will result in a reduction of E_F, and a consequent change of the density of states at E_F. In $U_xY_{1-x}Pd_3$, where non-Fermi-liquid behaviour is observed [11], the doping of Y^{3+} on the U^{4+} sites brings about a 'tuning' of the Fermi level [12]. The mixed valent nature of the U ions in UCu_5 is likely to reduce this effect in the present case.

This paper reports electrical resistivity, magnetoresistivity and magnetization measurements of $U_{1-x}Y_xCu_5$ at ambient pressure, over the concentration range $0 < x < 0.3$. In addition, we present resistivity measurements under hydrostatic pressure for certain concentrations. We have deduced a compositional phase diagram, plus a series of H–T and p–T phase diagrams, from our results. These diagrams are considered in the light of previous work in order to establish the influence of yttrium substitution on the degree of localization of uranium in this compound, and on the density of states at the Fermi level.

2. Experimental details

Polycrystalline samples of $U_{1-x}Y_xCu_5$ were prepared by arc melting in an argon atmosphere, and subsequently annealed under vacuum at 900 °C for two weeks. The starting materials were uranium and yttrium from Ames Laboratories (yttrium 99.99%) and copper (99.999%). X-ray powder diffraction measurements and SEM microprobe analysis revealed the samples to be single phase. Rietveld analysis was applied to the x-ray patterns, from which lattice parameters were deduced.

The samples used for resistance and magnetoresistance measurements were cut from the arc melted buttons by spark erosion. They had a typical cross-section of 1.50 mm by 1.50 mm and 3.00 mm between the voltage probes. We estimate that errors in measuring these dimensions, and non-uniformities in the sample cross-sectional area could lead to an error of $\pm 10\%$ in the absolute magnitude of the resistivities. The dc four terminal electrical resistance measurements were performed in London over the temperature range between 0.4 and 300 K at ambient pressure, with electrical contact being made with spring contacts. Measurements made between $T = 0.4$ and 80 K were performed using a top loading ^{3}He Oxford Instruments cryostat: the temperature was controlled and measured using Speer resistor and carbon glass sensors. This cryostat is fitted with a 12 tesla magnet, which enables the magnetoresistance to be measured over the 0.4–80 K range. Resistance measurements were also made on the same samples, from 4.2 to 300 K, using a dip-probe with a carbon glass thermometer. All the measurements were performed whilst heating the samples. The magnetoresistance measurements were performed after annealing the sample above the appropriate Néel temperature.

The pressure dependence of the resistivity was measured at T.U. Wien, again using the dc four terminal technique, with electrical contacts being established using indium solder in conjunction with an ultrasonic soldering iron. Hydrostatic pressure was applied using a clamp cell with a Teflon capsule, and the pressure transmitting medium was a mixture (4:1) of ethanol and methanol. The pressure was determined using two manometers, which ensured that the pressure was stable across the entire temperature range. All the measurements were made whilst heating.

The magnetization measurements were carried out at temperatures between 2 and 300 K using a Quantum Design SQUID magnetometer in London. The samples were cylindrical, having been spark eroded from arc melted buttons, and had a typical mass of 0.4 g. The measurements were made both heating and cooling in a magnetic field.

3. Results

In figure 1 we present results of the temperature dependent resistivity and magnetization of $U_{1-x}Y_xCu_5$ with $x = 0$, 0.05, 0.1 and 0.3. The measurements were all made for increasing temperature: the magnetization was measured in a magnetic field of 1 tesla. For $x = 0.05$ the results of the magnetization and resistivity resemble those obtained for pure UCu_5. However, the two transition temperatures have shifted with $T_N = 14.5$ K and $T_2 = 4.7$ K. For $x = 0.1$ only one transition is observed: it has an antiferromagnetic signature with $T_N = 11.4$ K. The sample with $x = 0.3$ shows a smooth decrease in the resistivity across the entire temperature range of $T = 4$ to 300 K. The magnetization also shows a similar trend down to approximately 10 K. In the figure there is a distinct anomaly at $T \sim 8$ K. A comparison of field cooled and zero-field cooled (not shown) measurements reveals that this anomaly has some associated hysteresis, which possibly indicates the onset of a frustration or freezing process.

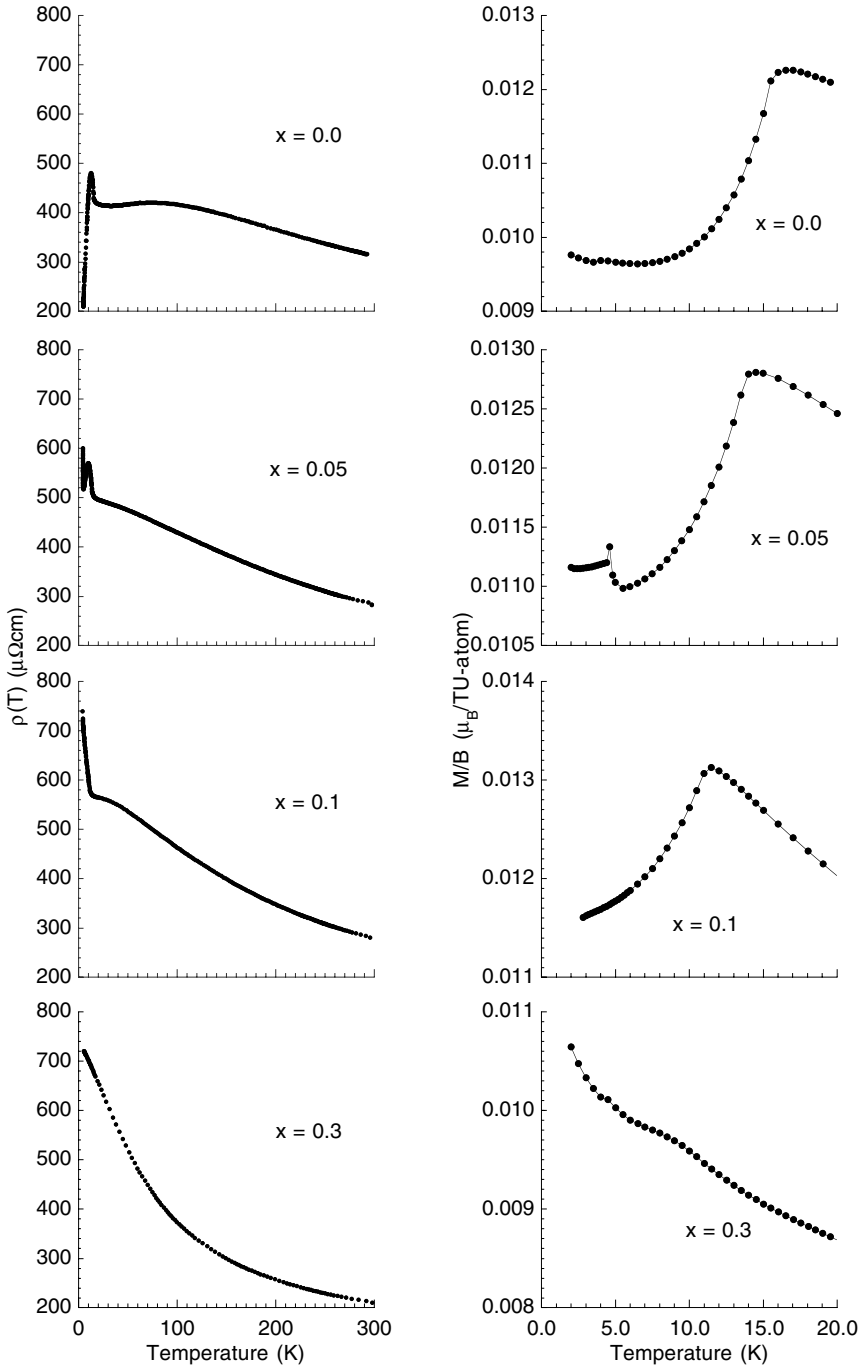

Figure 1. Temperature dependence of the zero field resistivity and dc susceptibility of $U_{1-x}Y_xCu_5$ measured at $\mu_0 H = 1$ T.

We have compiled a compositional phase diagram, figure 2, from the results of measurements in figure 1 and others made for varying yttrium concentration. The nomenclature

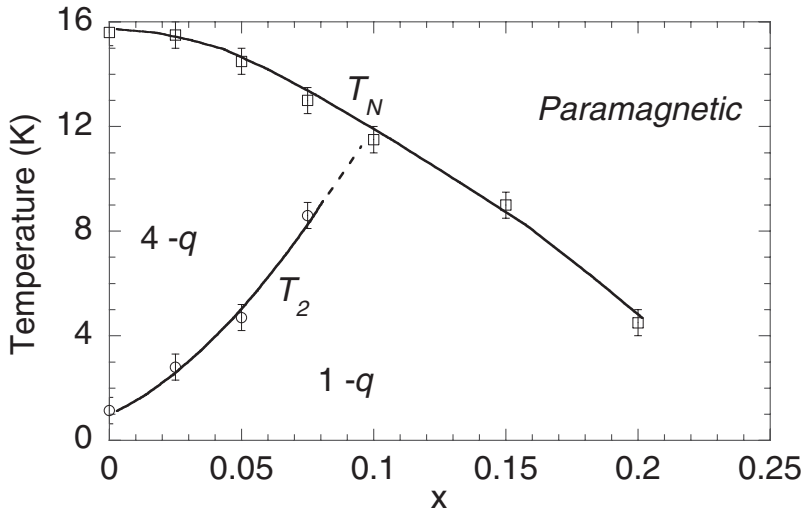

Figure 2. Compositional phase diagram for $U_{1-x}Y_xCu_5$ derived from a series of magnetization measurements. The nomenclature and description is discussed in section 4.

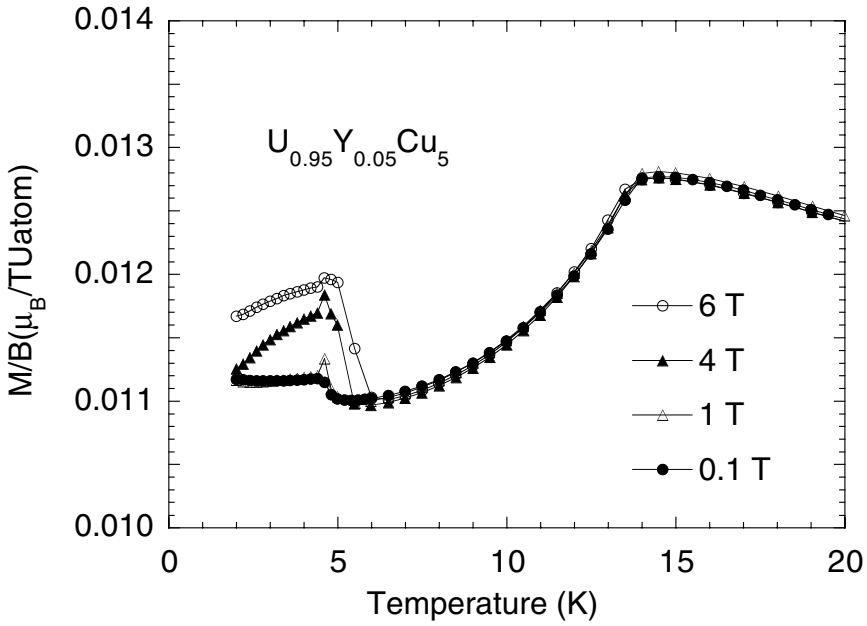

Figure 3. The magnetization at a series of dc fields for $U_{0.95}Y_{0.05}Cu_5$ and used to deduce magnetic phase diagrams presented in figure 9.

of the transitions and the magnetic structures have been extrapolated from those of pure UCu_5 [5], with arguments for this designation being presented in section 4.

Magnetization measurements, performed whilst heating, for $U_{0.95}Y_{0.05}Cu_5$ are presented in figure 3. At all fields we note the moments decrease dramatically at the transition T_2 from the $1-\boldsymbol{q}$ to $4-\boldsymbol{q}$ structure. This was observed in our earlier study [5] of UCu_5, where we found a similar 'frustration' of the moment in comparisons of measurements made after zero-field

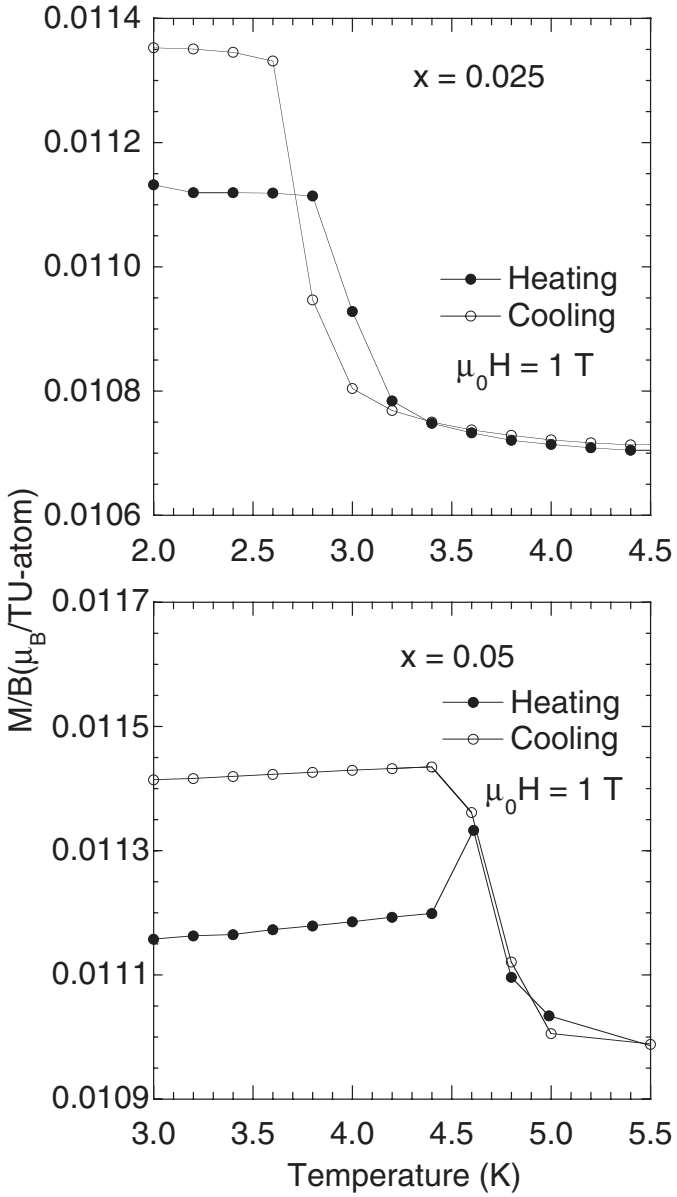

Figure 4. The magnetization of $U_{0.975}Y_{0.025}Cu_5$ and $U_{0.95}Y_{0.05}Cu_5$ revealing the development of hysteresis at T_2 as a function of yttrium concentration.

cooling and field cooling. In UCu_5 [5] there was a significant degree of hysteresis observed at T_2. In figure 4 we present evidence of hysteresis for the samples with $x = 0.025$ and 0.05. For $x = 0.025$ there is some evidence of hysteresis with $\Delta T \approx 0.17$ K, which is somewhat larger than that observed for pure UCu_5 where $\Delta T \approx 0.04$ K. However, for $x = 0.05$ there is little, if any, sign of hysteresis being present.

In figure 5 we present electrical resistivity and magnetoresistance measurements made over the temperature range $T = 0.4$–30 K. For $x = 0.025$ the form of the resistivity is similar

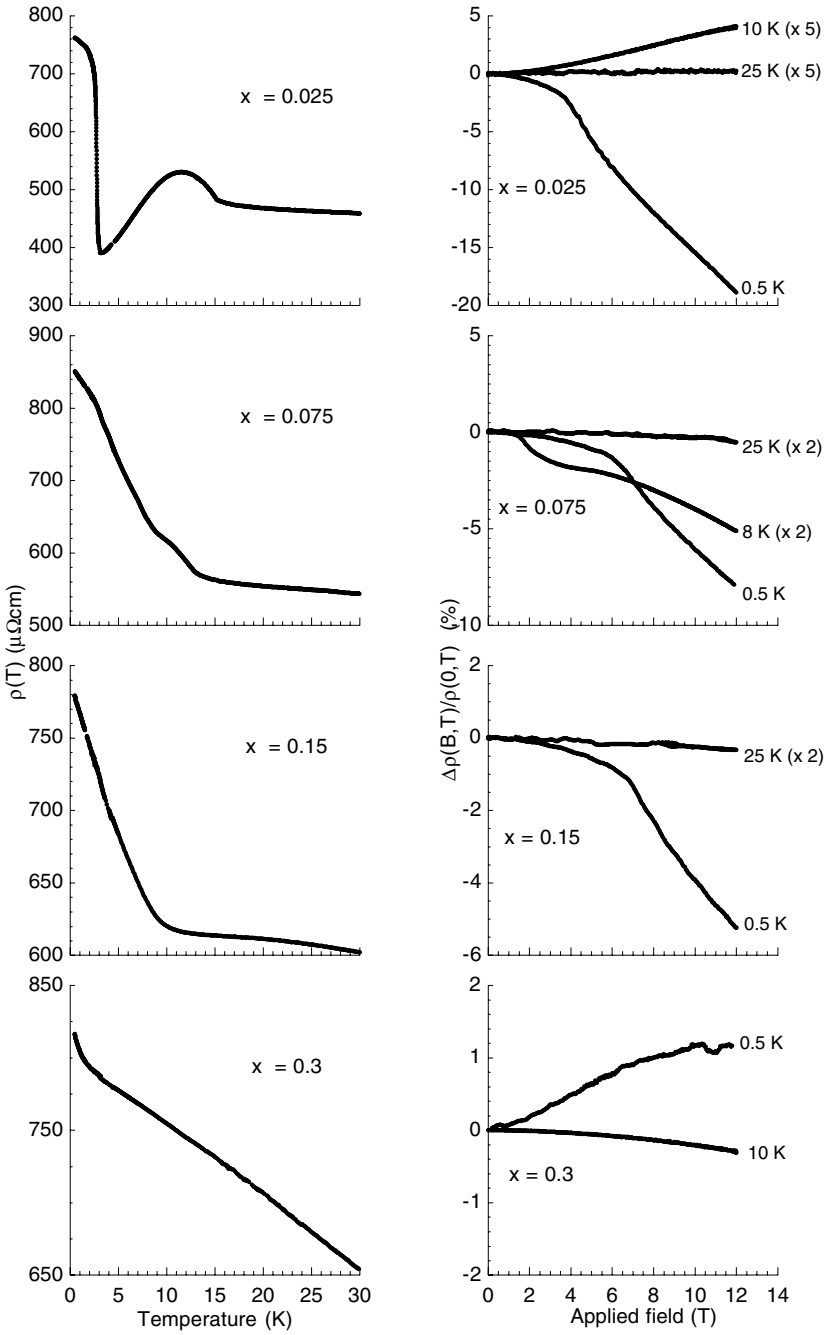

Figure 5. The resistance and magnetoresistance for $U_{1-x}Y_xCu_5$. All measurements were made after zero-field cooling from above the appropriate Néel temperature. The figures in parentheses are multiplying factors applied to the data in order to make trend visible.

to that observed for UCu_5 [5, 13]. At T_2 the resistivity increases by approximately 350 $\mu\Omega$ cm (from 400 to 750 $\mu\Omega$ cm) which is approximately 50% smaller than that observed for UCu_5

[1]. As the concentration of yttrium is increased we find that the two transitions begin to merge (figure 2), and at $x = 0.1$ the only transition detectable results in a large increase of the resistivity. This trend continues through to $x = 0.2$, but by $x = 0.3$ this is suppressed, with some evidence of an upturn at $T \approx 2$ K. The magnetoresistance on the right of figure 5 is illuminating. For $T = 0.5$ K and $x = 0.025$ to 0.15 the magnetoresistance has the same form with a sharp downturn at $\mu_0 H = 3$, 6 and 7 tesla respectively. The result for $x = 0.025$ may be contrasted with that observed [5, 13, 15] for UCu_5 where, below 2 tesla, the resistivity increases almost quadratically, and then decreases with an overall change of approximately 70% at 12 tesla. For $x = 0.025$ the overall decrease is 20% at 12 tesla, and there was no increase in the resistivity at any field. As the concentration of yttrium is increased we note that the decrease in the resistivity also reduces.

For $T = 10$ K there is a small increase in the resistivity of the $x = 0.025$ sample (note that the figures appearing in the brackets refer to multiplying factors used to make the data clearer). The magnetoresistance is reduced for this sample at $T = 25$ K. In the case of the sample $x = 0.075$ we observe a transition at approximately 2 tesla for $T = 8$ K with the resistivity decreasing further as the field increased. At 25 K the $x = 0.075$ and $x = 0.15$ samples show very little magnetoresistance for fields up to 12 tesla.

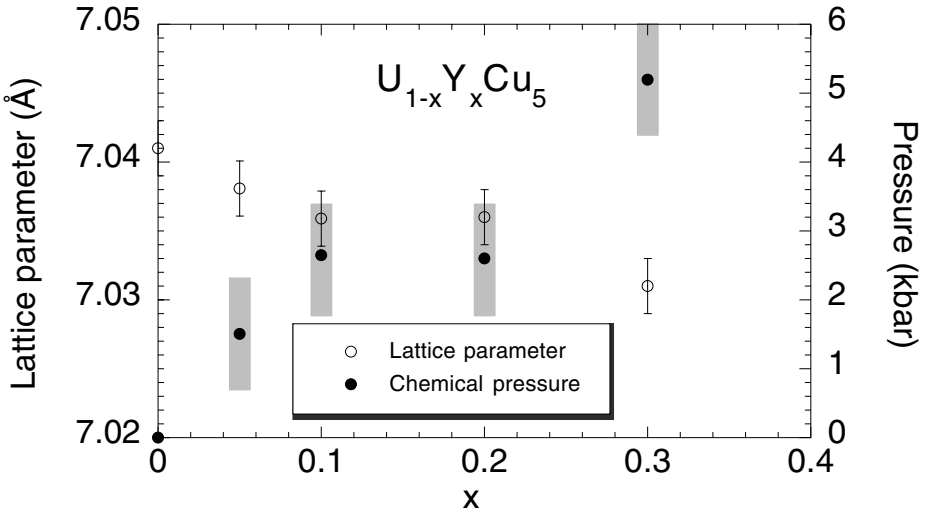

Figure 6. The lattice parameters derived from powder x-ray diffraction at room temperature for $U_{1-x}Y_xCu_5$ (open circles). The closed circles are the equivalent 'chemical' pressure derived using $B_T = 122$ GPa [17], and the shaded region indicates the associated error.

Table 1. Pressure derivatives for various alloys of UCu_5 derived from hydrostatic pressure measurements and chemical substitution.

	$\frac{dT_N}{dp}\|_{press}$ (K kbar^{-1})	$\frac{dT_N}{dp}\|_{chem}$ (K kbar^{-1})	$\frac{dT_N}{dp}\|_{press}$ (K kbar^{-1})	$\frac{dT_N}{dp}\|_{chem}$ (K kbar^{-1})
$U_{0.95}Y_{0.05}Cu_5$	+0.023	−0.6	−0.019	+2.4
$U_{0.925}Y_{0.075}Cu_5$	+0.009	−1.3	−0.069	+3.6
UCu_5	+0.034 [18]		−0.033 [18]	
UCu_5			−0.025 [14]	
UCu_4Ag	+0.032 [17]	−0.1 [6]		

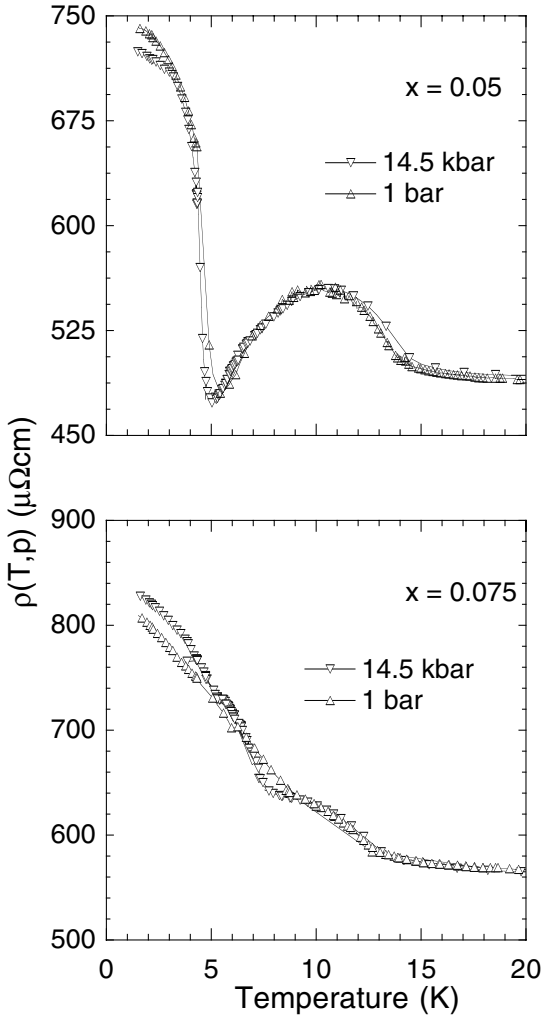

Figure 7. The temperature dependence of the resistivity for $U_{1-x}Y_xCu_5$ with $x = 0.05$ and 0.075. The measurements were made under hydrostatic pressures of 1 bar and 14.5 kbar.

The magnetoresistance for $x = 0.3$ is qualitatively different. At $T = 0.5$ K we observe an increase in the resistivity of approximately 1% at 12 tesla, and at $T = 10$ K the magnetoresistance is negative and similar to that observed in the paramagnetic state for the other samples studied.

In figure 6 we present the lattice parameter dependence on yttrium concentration. The graph shows both the lattice parameter and the equivalent change in pressure calculated using a bulk modulus (B_T) of 122 GPa determined for UCu_5 [16]. We see that the introduction of yttrium results in a small reduction of the cubic lattice, and the equivalent 'chemical' pressure is modest. Related to this figure is figure 7, which presents results of the electrical resistivity under hydrostatic pressure for two selected samples, $x = 0.05$ and 0.075. For $x = 0.05$ there is a small increase in the Néel temperature between 1 bar and 14.5 kbar, whilst T_2 shows a slight decrease across this pressure range. The sample $U_{0.925}Y_{0.075}Cu_5$ shows a similar trend, but T_2 reveals a stronger dependence on pressure.

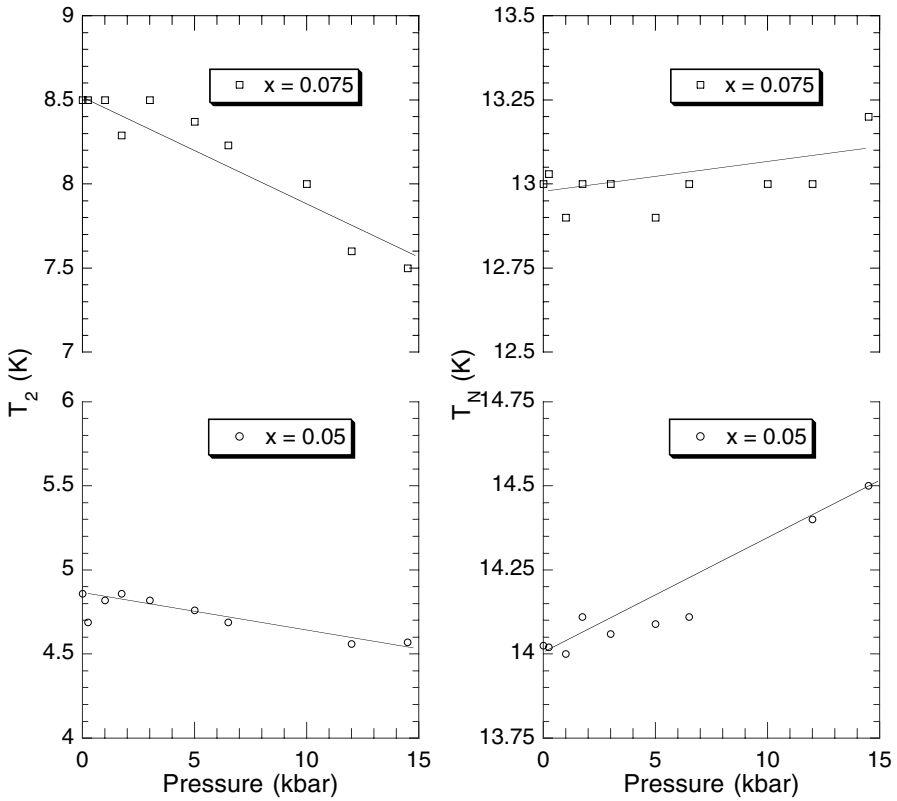

Figure 8. The p–T phase diagrams for $U_{0.95}Y_{0.05}Cu_5$ and $U_{0.925}Y_{0.075}Cu_5$ derived from series of measurements similar to those presented in figure 7. The nomenclature is discussed in section 4.

4. Analysis and discussion

4.1. The phase diagrams

In figure 8 we present the p–T phase diagrams for the compounds $U_{0.95}Y_{0.05}Cu_5$ and $U_{0.925}Y_{0.075}Cu_5$, showing a relatively weak dependence of the transitions on hydrostatic pressure. As indicated in the previous section, the change in lattice parameter associated with the substitution of uranium by yttrium may be viewed as the application of 'chemical' pressure. However, this interpretation must be treated with caution when considering the effects of the substitution. In figure 2 we observe that the effect of changing uranium concentration results in a dramatic change in the ordering temperatures. Figure 6 indicates the 'chemical' pressures resulting from the yttrium substitution. When we consider the phase diagrams in figure 8 we note that the effects of hydrostatic pressure are not comparable. In table 1 we present a summary of gradients dT/dp, in which results are compared between values derived from hydrostatic pressure, 'chemical' pressure and earlier studies. The sign of the gradients when comparing hydrostatic with 'chemical' pressure are opposite, and this difference is also apparent in the results for UCu_4Ag [17, 18]. This difference in sign implies that the influences of hydrostatic and chemical pressure are not analogous, indicating that the effects of yttrium substitution are not primarily associated with changes in the lattice volume. Care must be taken in considering the result for UCu_4Ag, since the effect of silver is to expand the lattice,

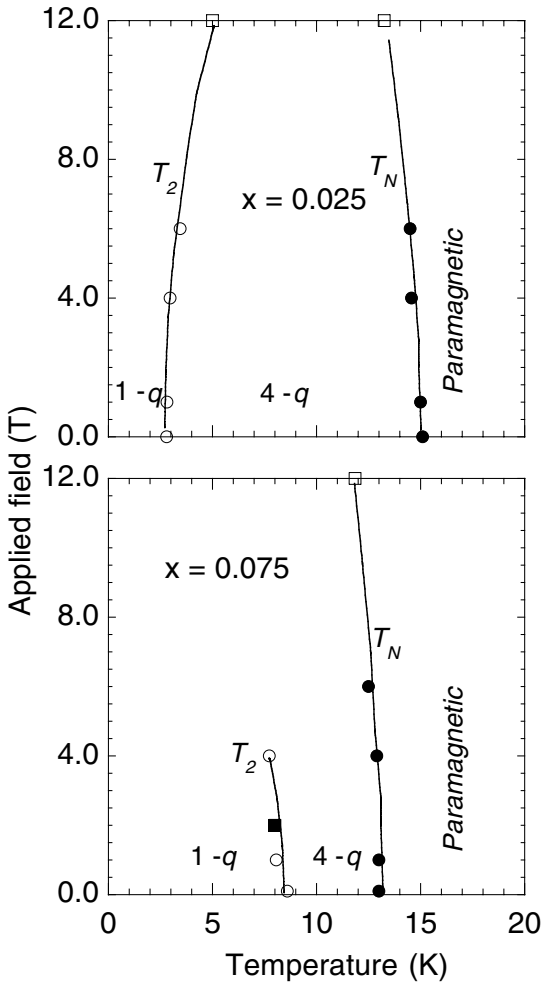

Figure 9. The H–T phase diagrams for $U_{1-x}Y_xCu_5$ with $x = 0.025$ and 0.075. The results of these phase diagrams are compared with those presented in figure 8, and discussed in terms of the entropy change.

which results in an increase of the Néel temperature. The other point of note in this comparison of the substitutional pressure and hydrostatic pressure is the magnitude of the gradients. For the $U_{1-x}Y_xCu_5$ samples the value of $dT/dp|_{chem}$ is almost an order of magnitude larger than that found for UCu_4Ag. The values derived using hydrostatic pressure for $U_{0.95}Y_{0.05}Cu_5$ are comparable with those observed for UCu_5 and UCu_4Ag, but those derived for $U_{0.925}Y_{0.075}Cu_5$ are clearly different. For example, the chemical pressure in the case of $x = 0.05$ is calculated to be 1.5 kbar and the change in the transition temperatures is large. However, the application of 14.5 kbar produces only small shifts in the transition temperatures and these shifts are in the opposite direction. This example highlights the differences that are taking place. Resonant photoemission studies [19] for UCu_5 reveal that the 5f electrons are strongly hybridized with the 3d electrons and therefore the valence state of U is intermediate between U^{3+} and U^{4+}. For Y the valence state can only be 3+ and there are grounds for suspecting that the change in the electronic state of the U ion may be responsible for the changes observed on substitution of yttrium. We will return to this discussion in the following subsection.

Using the magnetization, resistivity and magnetoresistance data, H–T phase diagrams were compiled for $x = 0.025$ and 0.075 and these are presented in figure 9. For the samples $U_{0.975}Y_{0.025}Cu_5$ and $U_{0.95}Y_{0.05}Cu_5$ the phase diagrams are similar to UCu_5 [5, 18]. The T_2 transition can be distinguished up to 12 T in $x = 0.025$, and clearly increases with increasing field. However, for $x = 0.075$, T_2 appears to decrease with field. Above 4 T the transition at T_2 is difficult to discern, hence the absence of data points. Nevertheless, we note from the data available for $U_{0.925}Y_{0.075}Cu_5$, the phase boundary at T_2 shows a different trend in $dH/dT_2 < 0$, though the moment decreases on heating through this transition, which suggests that the structure is similar to that observed at lower concentrations.

In our earlier study [5] of UCu_5 an analysis was made based on the Clausius–Clapeyron equation, $(dH/dT)_{trans} = -\Delta S/\Delta M$. In the present study we have the opportunity to make a similar analysis with a comparison made to the companion equation $(dp/dT)_{trans} = \Delta S/\Delta V$. We note here that the application of hydrostatic pressure must reduce the volume and thus $\Delta V < 0$. A comparison of the influence of hydrostatic pressure and applied magnetic field on the entropy reveals that for both samples the entropy change is the same whether deduced from pressure or field studies. In the case of UCu_5 [5], it was observed that the entropy decreased when applying a magnetic field, and we argued that this supported the transition from a $4 - \boldsymbol{q}$ to a $1 - \boldsymbol{q}$ structure. Here we observe the same changes in entropy and this supports the proposition that there is no significant change in the magnetic structures for the range of samples with $x = 0.075$.

In figure 2 we presented the compositional phase diagram associated with the change in yttrium concentration. The three main regions have been named paramagnetic, $4 - \boldsymbol{q}$ and $1 - \boldsymbol{q}$. It was argued [5] that in moving from the $4 - \boldsymbol{q}$ to the $1 - \boldsymbol{q}$ there will be a decrease in the entropy and this trend has been found to persist with increasing yttrium concentration. For this reason we suggest that the magnetic structures are the same, noting that neutron scattering measurements on polycrystalline samples are unable to distinguish between multidomain $1 - \boldsymbol{q}$ and single domain $4 - \boldsymbol{q}$ structures.

4.2. Resistivity and magnetization

The low temperature resistivity was presented in figure 5. For concentrations of yttrium up to $x = 0.2$ there are a number of features of note. For $x = 0.025$ there is a large increase in the resistivity on entering the $1 - \boldsymbol{q}$ state. This has been previously [14] attributed to a removal of Fermi surface as a consequence of the introduction of superzone boundaries [20]. In the instance of $x = 0.025$ there is an increase of 195%, similar to that observed in UCu_5 [14], but the absolute magnitude of the increase in [14] was approximately three times larger. The magnitude of $\Delta\rho$ decreases with x suggesting that the formation of superzones is impeded by the presence of yttrium impurities on the uranium site. For $x = 0.3$ there is a small upturn in the resistivity below 2 K. The process involved in this upturn is not connected with the development of the $1 - \boldsymbol{q}$ structure. This statement is based on the differences observed in the magnetoresistance shown in figure 5. For $x = 0.3$ the magnetoresistance is positive at $T = 0.5$ and may be attributed to the effects of the Lorentz force.

The magnetoresistance (figure 5) for $x = 0.025$ shows none of the trends found in earlier studies of UCu_5 [5, 13, 15], most notable of which is the high field magnetoresistance. In UCu_5 the magnetoresistance was approximately 70% [5] at 12 tesla, whilst for $x = 0.025$ it is barely 20%. It is suggested [5, 13] that the negative magnetoresistance is associated with the replacement of the Fermi surface as the moments flop or flip parallel to the applied field. Yamagishi *et al* [21] present a mechanism by which these spin rearrangements may occur in UCu_5. Their proposition is motivated by a magnetic phase diagram constructed from high-field

magnetization measurements. The field at which the first reorientation should take place is of the order of 11 tesla (at $T \sim 2$ K), and in the proposed scheme represents a turn of 25% of the moments in the $4 - \boldsymbol{q}$ structure. This study [21] did not extend into the temperature regime of the $1 - \boldsymbol{q}$ structure and no scheme was proposed, but the negative magnetoresistance of UCu_5 [5] does suggest a state similar to that of the $4 - \boldsymbol{q}$ structure. From these observations and the corresponding magnetoresistance at $T = 0.5$ K for $x = 0.025$ (and indeed $x = 0.05$ and 0.075) we may surmise that the $1 - \boldsymbol{q}$ structure is in some sense stabilized, requiring significantly higher magnetic fields to turn the moments. The magnetoresistance at 0.5 K for these three concentrations also reveals a change in gradient, the position of which moves to higher fields as x increases. At this stage it is not clear to what this may be attributed, but we note that the position of these transitions, when plotted with that observed for $x = 0$, reveals a $\mu_0 H \propto x^{1/2}$ relationship. We note that the transition observed for UCu_5 in [5] was at approximately 2 tesla and attributed to domain effects.

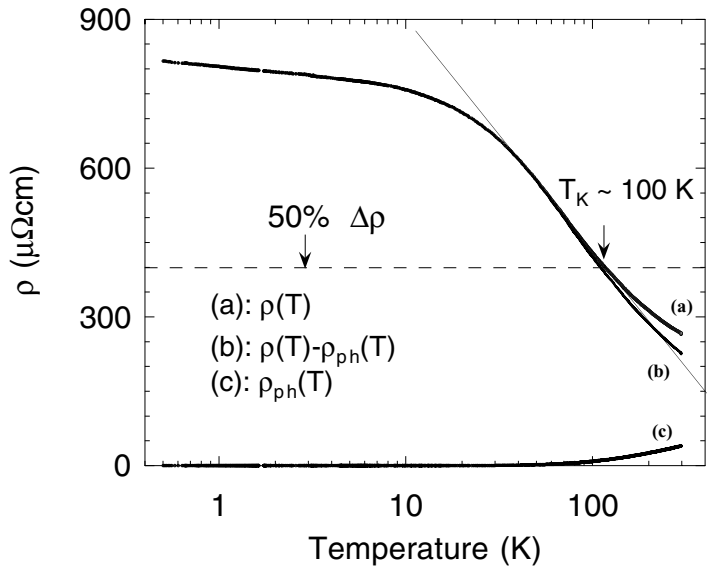

Figure 10. Estimation of the Kondo temperature for $U_{0.7}Y_{0.3}Cu_5$. Curve (a) is the uncorrected data, (b) is the data corrected for the phonon contribution derived from the Bloch–Grüneisen expression and the Debye temperature of UCu_4Ni [24]. Curve (c) is the phonon contribution.

At higher temperatures new features emerge, which highlight differences in the $x = 0.025$ and the 0.075 samples. For $x = 0.075$ at $T = 8$ K there is a transition centred at approximately 2 tesla, which may be identified on the appropriate magnetic phase diagram (figure 9). At this transition from the $1 - \boldsymbol{q}$ to the $4 - \boldsymbol{q}$ structure the resistivity decreases as the Fermi surface is replaced. However, as the field is increased the resistivity is observed to decrease in the $4 - \boldsymbol{q}$ structure. The model proposed by Yamada and Takada [22] would suggest that this is attributable to a suppression of spin fluctuations and a consequent reduction in scattering. The alloy with $x = 0.025$ at a temperature $T = 10$ K is in a $4 - \boldsymbol{q}$ magnetic structure. However, as the applied magnetic field is increased the resistivity increases. This increase can be interpreted [22] as arising from an enhancement of the scattering as the moments are aligned by the magnetic field. This difference in response of the magnetoresistance suggests that there is some fundamental difference in the nature of the magnetic structure of these two

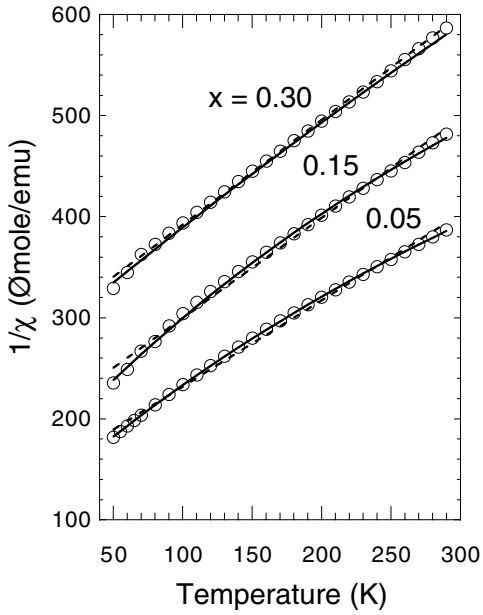

Figure 11. Fits to $1/\chi$ performed for $x = 0.05$, 0.15 and 0.30 over the temperature range $T = 50$ to 290 K. The solid and dashed curves represent the fits to data with and without the inclusion of χ_0 respectively.

compounds in the region nominally described as $4 - \boldsymbol{q}$. This result may be interpreted as a weakening of the anisotropy field as the concentration increases; this would explain the ease with which the moments are turned.

The discussion above relates to that portion of the phase diagram (figure 2) showing clear magnetic transitions. $U_{0.7}Y_{0.3}Cu_5$ in contrast, shows paramagnetic behaviour, but its resistivity (see figure 1) does not show conventional metallic behaviour and is similar to that observed for UCu_4Pd [7] or UCu_4Ni [8]. The resistivity of these latter materials show non-Fermi-liquid behaviour and departs from a T^2 dependence at low temperatures. The increase in resistivity of UCu_4Pd and UCu_4Ni across much of the temperature range has been accounted for using a Kondo disorder model [9, 23]. In figure 10 we present the resistivity plotted as a function of log T curve (a), and this reveals a Kondo-like behaviour. In this figure we present the data with the phonon contribution subtracted in curve (b), and from this we estimate a value of T_K of approximately 100 K. The phonon contribution was estimated using the high temperature resistivity with a linear (phonon) and a Kondo contribution. From the value of resistivity at room temperature and the Debye temperature, scaled from that of isostructural materials [24], the Bloch–Grüneisen phonon contribution was calculated (see curve (c) of figure 10). The question remains as to whether this system may be represented by a Kondo impurity model or a Kondo disorder model. The x-ray analysis revealed that the yttrium was situated on the uranium sites of the lattice. This structure has only one position for the U and thus as we dope the compound with yttrium we will be doing so randomly, creating a lattice of random spin centres. The Kondo disorder model requires that the magnitude of the spin from one site to the next has some distribution and the Kondo temperature therefore has some spread of values, this spread is assumed to be Gaussian. In the case of UCu_4Pd [7] it is suggested that the local environment of the uranium brings about the changes in magnitude of the spin.

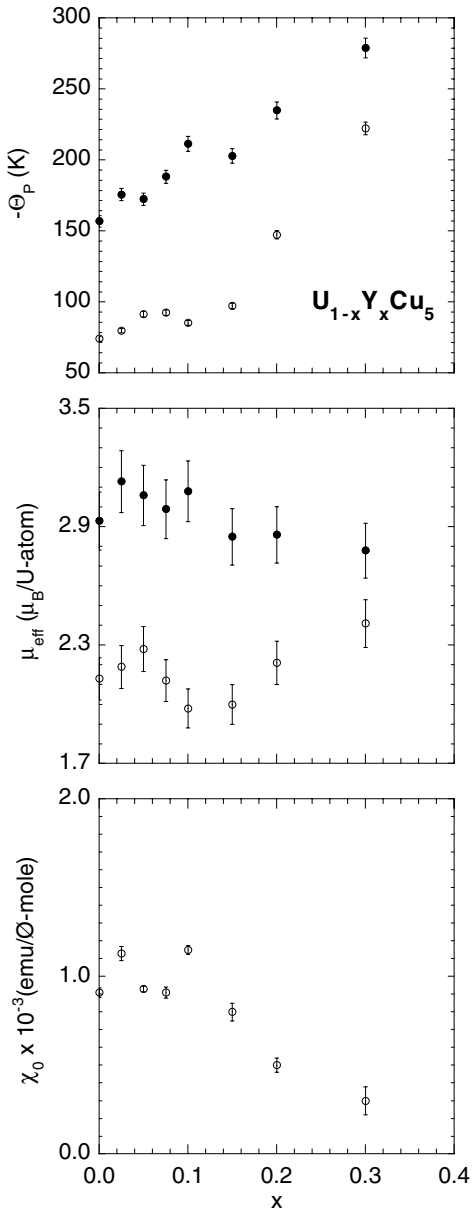

Figure 12. The fit parameters deduced from the application of equation (1) to the paramagnetic susceptibility of $U_{1-x}Y_xCu_5$. The open circles include χ_0 and the closed circles are without χ_0. The top panel presents the paramagnetic Curie–Weiss temperature. The central panel represents the trend in the effective paramagnetic moment whilst the panel at the bottom shows the trend in χ_0 as a function of x.

To establish whether yttrium leads to disorder of the local moment on the uranium sites we need to establish that the yttrium influences the moment. In order to do this we made an analysis of the data between $T = 50$ and 300 K using the equation

$$\chi = \frac{C}{T - \Theta_P} + \chi_0. \tag{1}$$

The extra term, χ_0, is included to encompass the possibility of a Pauli contribution or magnetic impurities. In figure 11 we present results of such fits for $x = 0.05$, 0.15 and 0.30. The solid and dashed curves represent fits with $\chi_0 \neq 0$ and $\chi_0 = 0$, respectively. We observe that equation (1) provides a closer fit. The fit parameters from this analysis are presented in figure 12, where the open circles represent the fit with $\chi_0 \neq 0$ and the closed circles represent the results of analysis with $\chi_0 = 0$. The top graph shows the dependence of the paramagnetic Curie–Weiss temperature, Θ_P. The analysis using both methods reveals that Θ_P is enhanced by the inclusion of yttrium in the lattice. However, with the inclusion of the additional temperature independent term, the value of Θ_P remains approximately constant until $x = 0.15$, thereafter the magnitude increases. The sign of Θ_P is negative in both analyses and indicates the presence of antiferromagnetic correlations. The middle figure presents the paramagnetic moment. With the inclusion of χ_0, the effective moment remains almost constant at approximately 2.3 μ_B U atom with increasing yttrium concentration. With the exclusion of χ_0, the moment is found to remain unchanged with x, and has a value of approximately 2.9 μ_B U atom for $x = 0.3$ (for a free uranium $5f^2$ ion 3.58 μ_B U atom). The lower graph in figure 11 presents the concentration dependence of χ_0. As indicated earlier, the physical origins of this component can derive either from an component due to the Pauli susceptibility or some ferromagnetic impurity. If the χ_0 contribution derives from a magnetic impurity, there would be a smooth decrease in χ_0 with increasing yttrium concentration. However, χ_0 is observed to be insensitive to changes in yttrium concentration up to $x = 0.1$. For $x > 0.1\chi_0$ is observed to decrease with increasing yttrium concentration. This suggests that χ_0 is not an impurity effect and derives from a temperature independent Pauli term: this term is directly related to density of states at the Fermi surface ($N(E_F)$). The value of χ_0 has been studied in heavy fermion systems and normal metals. For example $CeCu_6$ has [25] been found to have a value of $\chi_0 = 27 \times 10^{-3}$ emu $\varnothing^{-1}$ mol^{-1}, whilst UPt_3 has [26] a value of $\chi_0 = 7 \times 10^{-3}$ emu $\varnothing^{-1}$ mol^{-1} and in Pd $\chi_0 = 0.7 \times 10^{-3}$ emu $\varnothing^{-1}$ mol^{-1} [27]. The values derived here for $U_{1-x}Y_xCu_5$ fall in the range 0.3 to 1.0 $\times 10^{-3}$ emu $\varnothing^{-1}$ mol^{-1}. The trend of for $x = 0$ and 0.1 is nearly constant, whilst there is a decrease of nearly 70% in χ_0 for $0.1 < x < 0.3$. In the latter region we note from figure 2 that this corresponds to a sharp decrease in T_N where the magnetic structure formed is the $1 - \boldsymbol{q}$ modulated structure. It was argued earlier that the transition to the $1 - \boldsymbol{q}$ resulted in the formation of superzone boundaries and such a transition would result in a loss of Fermi surface. Since χ_0 is directly related to the density of states at the Fermi surface a reduction in χ_0 is consistent with a stabilization of the $1 - \boldsymbol{q}$ structure.

5. Conclusions

The decrease of the value of T_N in $U_{1-x}Y_xCu_5$ as x increases does not derive from any effect due to chemical pressure resulting from a change in the uranium concentration, and is much stronger than expected from a simple dilution. A comparison of the magnetoresistance for $x = 0.025$ and 0.075 in the $4-\boldsymbol{q}$ structure suggests that there is a weakening of the coupling as x increases, and this is also suggested by the decrease of T_N with x. It is not clear whether this is through the exchange field or the anisotropy field. From an analysis of the paramagnetic susceptibility using equation (1) we derive values for χ_0 which show only a weak concentration dependence for the concentration range $x = 0$ to 0.1. The magnetoresistance measurements (figure 5) for $x = 0.025$ suggest that the various magnetic structures are in some sense stabilized, and the formation of magnetic domains may be impeded by the introduction of yttrium into the lattice. Figure 4 shows that the hysteresis at T_2 is at a maximum for $x = 0.025$ whilst for $x = 0.05$ there is no significant hysteresis observed which implies that the transition at T_2 has become second order. Figure 1 shows that the moment at the Néel transition is largest for $x = 0.1$.

All these observations support the view that the moment on the uranium site is stabilized with increasing yttrium concentration.

The trend in the Pauli susceptibility (χ_0) suggests that there is a significant change in the density of states ($N(E_F)$) at the Fermi surface for $x > 0.1$ and this decrease in $N(E_F)$ can explain the magnitude of the resistivity observed for $x = 0.3$. It is noted that the resistance at room temperature for $U_{0.7}Y_{0.3}Cu_5$ is approximately 40% lower than that observed for UCu_5 at the same temperature and this is consistent with a reduction of $N(E_F)$. This being the case, the mobility of the conduction electrons in $U_{0.7}Y_{0.3}Cu_5$ will be enhanced over that found in the heavy fermion state observed in the parent compound. The resistivity of $U_{0.7}Y_{0.3}Cu_5$ shows a negative temperature coefficient. The plot of the paramagnetic Curie–Weiss temperature as a function of increasing yttrium concentration in figure 11 shows an increase for $x > 0.1$. If we assume that this derives from a Kondo process, with $T_K = \Theta_P/2$ [28], then we deduce from this expression that $T_K \approx 100$ K for $U_{0.7}Y_{0.3}Cu_5$ and this is consistent with the value derived from figure 10. In making this analysis of the susceptibility there has been no inclusion of a contribution from the crystal field. A literature survey for UCu_5 revealed that no work has been reported for crystal field studies on this compound. This does not, however, rule out the possibility that such a contribution exists. This aspect will require a further investigation for both the parent compound and the doped compounds.

The application of hydrostatic pressure in these compounds and earlier studies [17, 18] increases T_N. The mechanism by which this occurs has not been explained. If we assume that the resistivity increase on approaching T_N from above is a consequence of some Kondo mechanism then we would assume that, in the absence of magnetic order, this system would form a Kondo lattice at some particular temperature. The signature for such an event would be a marked decrease in the resistivity. In UCu_5, and these compounds, there is a saturation of the resistivity as a precursor to magnetic order, and in fact a broad maximum is observed (figure 1, $x = 0$) in the resistivity centred at approximately 70 K. On the basis that these fluctuations in the spin are antiferromagnetic ($\Theta_P < 0$), it is not unreasonable to suggest that the application of pressure would assist in creating correlations in these fluctuations and consequently result in an increase of the ordering temperature T_N. However, we cannot rule out the possibility of metallurgical problems associated with the compound UCu_5.

Acknowledgments

M Watmough thanks the UK Engineering and Physical Sciences Research Council for a research studentship. We acknowledge the assistance of M Arranz for related measurements of Debye temperature, A Beard for SEM measurements and J Cockcroft for x-ray diffraction measurements. We acknowledge the Austrian FWF, project P12899, for supporting the high pressure studies in Wien. Finally we acknowledge the European Science Foundation, FERLIN project, for travel grants received.

References

[1] Ott H R, Rudigier H, Felder E, Fisk Z and Batlogg B 1985 *Phys. Rev. Lett.* **55** 1595
[2] Murasik A, Ligenza S and Zygmunt Z 1974 *Phys. Status Solidi* a **23** K163
[3] Schenck A, Birrer P, Gynax F N, Hiiti B, Lippelt E, Weber M, Böni P, Fisher P, Ott H R and Fisk Z 1990 *Phys. Rev. Lett.* **65** 2454
[4] Nakamura H, Kitaoka Y, Asayama K, Onuki Y and Shiga M 1994 *J. Phys.: Condens. Matter* **6** 10 567
[5] Lopez de la Torre M A, McEwen K A, Ellerby M, Haworth C and Springford M 1995 *J. Phys.: Condens. Matter* **7** 9235
[6] McEwen K A, Lopez de la Torre M A, Watmough M and Ellerby M 1997 *Physica* B **230–232** 59

[7] Andraka B and Stewart G R 1993 *Phys. Rev.* B **47** 3208
[8] van Daal H J, Buschow K H J, van Aken P B and van Maaren M H 1975 *Phys. Rev. Lett.* **34** 1457
[9] Bernal O O, McLaughlin D E, Lukefahr H G and Andraka B 1995 *Phys. Rev. Lett.* **75** 2023
[10] López de la Torre M A, Ellerby M, Watmough M, McEwen K A 1998 *J. Magn. Magn. Mater.* **177–181** 445
[11] Seaman C L, Maple M B, Lee B W, Ghamaty S, Torikachvili M S, Kang J-S, Liu L Z, Allen J W and Cox D L 1991 *Phys. Rev. Lett.* **67** 2882
Andraka B and Tsvelik A M 1991 *Phys. Rev. Lett.* **67** 2886
[12] Kang J-S, Allen J W, Maple M B, Torikachvili M S, Ellis W P, Pate B B, Shen Z-X, Yeh J J and Lindau I 1989 *Phys. Rev.* B **39** 13 529
[13] Ott H R, Felder E and Bernasconi A 1993 *Physica* B **186–188** 207
[14] Bruls G, Joss W, Welp U, Ott H R, Fisk Z, Cors G and Karkut M 1987 *J. Magn. Magn. Mater.* **63–64** 181
[15] Onuki Y, Yamazaki T, Ukon I, Komatsubara T, Sato H, Sugiyama Y, Sakamoto I and Yonemitsu K 1988 *J. Physique Coll.* **49** C8-481
[16] Venter A M, de v du Plessis P and Smit P 1997 *Physica* B **230–232** 59
[17] Thompson J D, Fisk Z and Ott H R 1986 *J. Magn. Magn. Mater.* **54–57** 393
[18] Thompson J D 1987 *J. Magn. Magn. Mater.* **63/64** 358
[19] Schneider W D, Reihl B, Mårtensson N and Arko A J 1982 *Phys. Rev.* B **26** 423
[20] Mackintosh A R 1962 *Phys. Rev. Lett.* **9** 90
[21] Yamagishi A, Senda K, Kindo K, Date M and Onuki Y 1992 *J. Magn. Magn. Mater.* **108** 211
[22] Yamada H and Takada S 1973 *Prog. Theor. Phys.* **49** 1401
[23] Lopez de la Torre M A, Izquierdo A, Vieira S, Ellerby M and McEwen K A 2000 *J. Appl. Phys.* **87** 5126
[24] Lopez de la Torre M A, Arranz M, Ellerby M and McEwen K A 2001 to be published
[25] Stewart G R, Fisk Z and Wire M S 1984 *Phys. Rev.* B **30** 482
[26] Frings P H, Franse J J M, Smith J L and Fisk Z 1983 *J. Magn. Magn. Mater.* **63/64** 240
[27] Hoare F E and Matthews J C 1952 *Proc. R. Soc.* A **212** 137
[28] Blanco J A, de Podesta M, Espeso J I, Gómez Sal J C, Lester C, McEwen K A, Patrikios N and Rodríguez Fernández J 1994 *Phys. Rev.* B **49** 15 126